Review

Progress towards automated diabetic ocular screening: a review of image analysis and intelligent systems for diabetic retinopathy

T. Teng **M. Lefley** **D. Claremont**

Academic Biomedical Engineering Research Group, School of Design, Engineering & Computing, Bournemouth University, Dorset, UK

Abstract—*Patients with diabetes require annual screening for effective timing of sight-saving treatment. However, the lack of screening and the shortage of ophthalmologists limit the ocular health care available. This is stimulating research into automated analysis of the reflectance images of the ocular fundus. Publications applicable to the automated screening of diabetic retinopathy are summarised. The review has been structured to mimic some of the processes that an ophthalmologist performs when examining the retina. Thus image processing tasks, such as vessel and lesion location, are reviewed before any intelligent or automated systems. Most research has been undertaken in identification of the retinal vasculature and analysis of early pathological changes. Progress has been made in the identification of the retinal vasculature and the more common pathological features, such as small aneurysms and exudates. Ancillary research into image preprocessing has also been identified. In summary, the advent of digital data sets has made image analysis more accessible, although questions regarding the assessment of individual algorithms and whole systems are only just being addressed.*

Keywords—*Diabetic retinopathy, Image processing, Screening, Automation, Intelligent systems, Fundus image analysis*

Med. Biol. Eng. Comput., 2002, **40**, 2–13

1 Introduction

OBJECTIVE DIAGNOSTIC indices in diabetic retinal health care have been studied since 1969 (SKOVBORG *et al.*, 1969). This review summarises the published literature on image processing and automated systems for the screening and diagnosis of diabetic retinopathy (DR). It focuses on image processing algorithms for the segmentation (i.e. the identification) of the retinal anatomy and the lesions induced by diabetes mellitus.

The medical, social and financial rationale supporting regular and frequent screening for the lesions of DR is strong. Detailed and well-documented diagnostic protocols have been developed over the last 20 years (DRS RESEARCH GROUP, 1981; ETDRS RESEARCH GROUP, 1991*a*). It is important to note that timely treatment for DR prevents severe visual loss in over 50% of eyes (ETDRS RESEARCH GROUP, 1985; 1991*b*; DRS RESEARCH GROUP, 1987).

Computer simulations of recommended eye care (AMERICAN DIABETES ASSOCIATION, 1999), performed by JAVITT *et al.* (1994) and DASBACH *et al.* (1991), demonstrated that prevention and treatment were less expensive than the health care and rehabilitation costs incurred by visual loss or blindness. In spite of this evidence, there is still a need for structured care to impart these potential benefits in the United Kingdom (DIABETES UK, 2000; NATIONAL SCREENING COMMITTEE, 2000). A comprehensive medical overview of DR, including the data required for optimum care, can be found in AIELLO *et al.* (1998*a*).

Current retinal image databases are not sufficiently integrated with hospital information systems to allow correlations between the patient's condition and novel features of the retinal images to be investigated. Instead, research locating or measuring individual anatomical landmarks or specific diabetic pathology is receiving the most attention. Previous papers that review the image processing of retinal image data exist (GOLDBAUM *et al.*, 1990*a*; WARD *et al.*, 1988), but these need updating to include a decade of research. It should also be noted that many studies lack objective results and so cannot be quantitatively evaluated.

Correspondence should be addressed to Prof. D. Claremont; email: dclaremo@bmth.ac.uk

Paper received 11 May 2001 and in final form 17 September 2001

MBEC online number: 20023645

2 Image processing for segmentation of the normal retina

From colour transparencies and digital images of the retina, the optic disk, vessels and retinal parenchyma are easily recognised (see Fig. 1). These landmarks give a framework

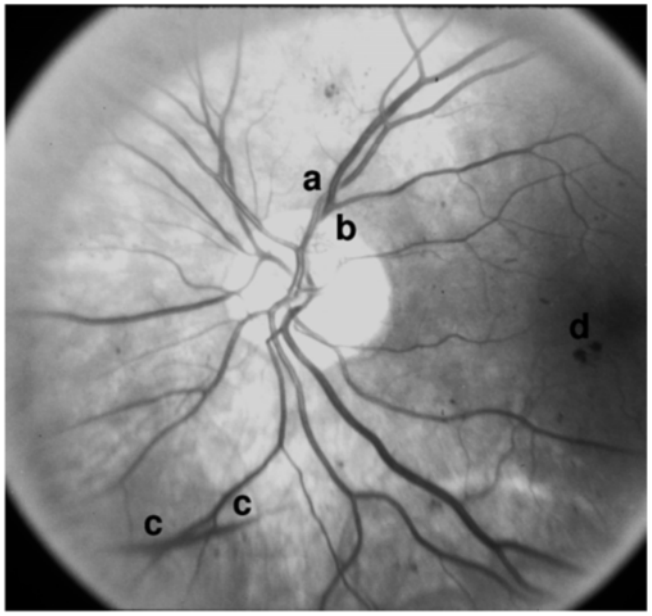

Fig. 1 *Standard image 10A from ETDRS grading scheme. Note variability of contrast due to retinal pigment and imaging. Optic disk (bright circular feature in centre) has (a) twisted artery and vein at its rim and (b) small tuft of neovascularisation within it. (c) Preretinal haemorrhage and (d) intra-retinal haemorrhages are also apparent*

from which automated analysis and human interpretation of the retina proceed. However, the image must be of adequate quality and resolution.

2.1 *Image resolution*

A monochrome digital image can be represented as a two-dimensional array, with each cell or picture element (pixel) holding a value representing the intensity at that point in the image. This intensity is also called the grey level and is usually limited in resolution by the number of bits (or bytes) that represent it.

The spatial resolution of a digital image is given by its area in pixels, their size and the field of view. For a fundus image recorded on photographic film and through clear ocular media, the resolving power of the whole system is limited by the film and its development. The spatial resolution of typical transparency film used for imaging DR ranges from 1 to 100 cycles mm^{-1} for a response above 10%.*

Film resolutions of approximately 4000 $pixel^2$ have been quoted by SCHALKOFF (1989). This figure is of the same order of magnitude as the 50–130 lines mm^{-1}, or 4600 lines per 35 mm, quoted by the Agfa datasheets. Film-based evaluation of DR uses a relatively small or narrow field of view. For 35 mm film-based stereoscopic evaluation, two 30° field of view images are required. Lesions of the retinal capillaries, such as micro-aneurysms and intra-retinal microvascular abnormalities (IRMA) require this resolution for unequivocal assessment.

Digital image acquisition is usually over a larger field of view; with 45, 50 or 60° being typical. Images are usually rectangular and have the long dimension ranging from 600 to 1024 pixels. Digital images thus represent larger fundus areas at lower resolutions. The film-based reference imaging protocol also uses stereoscopic pairs that the interpreter could integrate to advantage. Digital transducers have linearity and sensitivity advantages over photographic film. The ease and fidelity of reproduction and transmission mean that digital imaging will become an attractive alternative to 35 mm film-based methods, once the resolution approaches that of traditional film.

*Data obtained from Kodak, Agfa and Fujifilm websites for Ektachrome, Agfachrome and Fujichrome transparency films

2.2 *Image preprocessing*

Patient movement, poor focus, bad positioning, reflections, disease opacity or inadequate illumination can cause a significant proportion of images to be of such poor quality as to interfere with analysis. The sphericity of the eye, a significant determinant in the intensity of reflections from the retinal tissues, compounds artifacts such as circular and crescent-shaped low-frequency contrast and intensity changes arising from the interface between the anterior and posterior ocular chambers.

In approximately 10% of retinal images, artifacts are significant enough to impede human grading (KRISTINSSON *et al.*, 1997; KLEIN *et al.*, 1989; LIESENFELD *et al.*, 2000). A similar proportion is presumed to be of inadequate quality for automated analysis. Preprocessing of the fundus data either removes or flags the aforementioned interferences. LEE and WANG (1999) proposed that, by correlating the histogram of intensities of an image with that of an ideal histogram representing the best images, an index describing the contrast, brightness and signal-to-noise ratio of an image could be obtained. The authors describe their results as being in agreement with human perceptions.

OKAZAKI and TAMURA (1983) approximated unequal retinal illumination as spherical. Their surface fitting algorithm was successfully applied to the image after a range of thresholds had been set. The average centre of these binary images provided enough terms to apply a least squares method to find the radius and vertical offset. LEE (1992) found median filtering to be preferable to the fitting of high-degree polynomials, reasoning against non-linear computations and the parameter selection involved. LEE (1992), ØIEN and OSNES (1995), MENDONÇA *et al.* (1999), SHIN *et al.* (1999) and EGE *et al.* (2000) used a 31 $pixel^2$ median filter as a smoothing operator to remove the effect of the background. Other background changes introduced during film digitisation have been removed by subtracting (FRAME *et al.*, 1997*a*;*b*) or dividing (CREE *et al.*, 1997) the uneven illumination known as the flood image.

Some information about retinal images is commonly discarded before image processing. During colour digital image acquisition, the intensities of the reflected illumination are recorded at three wavelengths. These three wavelengths are chosen to represent the red, green and blue (RGB) spectral ranges of the human photosensitive pigments. Sometimes, only the the green band is used in the image processing of digital retinal images (CHAUDHURI *et al.*, 1989*a*; GOLDBAUM *et al.*, 1989; KOCHNER *et al.*, 1998; MARTÍNEZ-PÉREZ *et al.*, 1999*a*; LEE *et al.*, 1999; ZAHLMANN *et al.*, 2000).

The spectral content of each pixel can be decoupled from its intensity measure, and, with this approach, it is possible to operate independently on either brightness values or its perceived colour. SINTHANAYOTHIN *et al.* (1999) used the hue, intensity, saturation colour space described by GONZALEZ and WOODS (1992) to perform a local sigmoidal histogram stretch on the intensity plane. This increased the local contrast and minimised contrast variations over the whole image. Alternatively, shading and illumination anomalies can be ignored in small regions of interest or sub-windows (AKITA and KUGA, 1979; GREGSON *et al.*, 1995).

2.3 *Locating and segmenting the optic disk*

The optic disk (OD) is the brightest feature of the healthy fundus; it is approximately circular and measures $\approx 1800\mu m$ in diameter; the retinal vasculature originates from its centre (see

Fig. 1). The OD lacks a visible capillary supply and appears paler owing to the lack of an underlying pigmented layer.

The contrast between the emerging translucent, blood-filled vessels and the white background was exploited by SINTHANAYOTHIN *et al.* (1999). They used a local measure of pixel intensity variance, of window size equal to that of the OD (80 pixels), and swept it over the image. The measured peak variance was successful in locating the OD in 111 out of 112 test images.

Instead of the variance, the average brightness value alone has also been used to locate the OD (LEE *et al.*, 1999; TAMURA *et al.*, 1988). A combination of many features, such as edge concentration, colour and brightness, was weighted by KATZ *et al.* (1988) to highlight regions with OD-like properties. CHAUDHURI *et al.* (1989*b*) used local measures of vessel convergence and orientation combined with a matched filter for bright circular objects to locate the optic disk. This resulted in OD localisation of 31 optic disks in 35 predominantly pathological images.

The convergence of the retinal vessels upon the OD was more exhaustively exploited by HOOVER and GOLDBAUM (1998*a*) and AKITA and KUGA (1982). The latter study identified the order in which the vessels branch from the OD origin and measured the intensity of the fundus around this ranked list. The brightest pixel in the neighbourhood of the highest ranked, or root, vessel was then identified as the OD centre. HOOVER and GOLDBAUM (1998*a*) used elongated and smeared versions of vessel segements. The now diffuse vessels accumulated and overlapped in areas of convergence, such as the optic disk.

The Hough transform, a method for locating basic shapes such as circles and lines, was used by KOCHNER *et al.* (1998) to locate the optic disk. They segmented the two main vascular arches to obtain points to which an ellipse was fitted. At the apices of this ellipse, the OD was prospectively located using matched filters (see Section 2.4.2) to find the major vessels leaving the OD. The response of the matched filters was maximum if radially distributed vessels were present within a bow-tie shaped region of interest (ROI), centred on the presumed location of the optic disk. A Hough transform for circular feature detection has also been employed (YULONG and DINGRU, 1990). The edge points were derived from the whole image using a series of transformations aimed at detecting the bright optic disk.

WANG *et al.* (1990) fitted circles to the OD by successive approximation. Their approach started with an unspecified thresholding. Pixels were iteratively rejected from the resulting binary image by the discarding of 15% of pixels not within a shrinking circle centred on the mean location. If, after shrinking, the origin of the circle could not be moved so as to reject a further 15% of pixels not within the circle, the OD was taken to be identified.

2.4 *Segmentation of the retinal vasculature*

This Section summarises research into segmenting or deriving a binary image representing the retinal vasculature. The approaches are varied, and the *a priori* knowledge is substantial, and yet the results are scarce. The vascular tree needs to be segmented so that its physical dimensions can be measured. Length, diameter and path, and the changes induced by the progression of DR, can become valuable diagnostic indices of the disease. Vascular segmentation is also required to stop the curvilinear shapes from interfering with subsequent analysis of DR lesions.

Most of the results published for vascular segmentation are described as adequate or presented as side-by-side comparisons. An algorithm should be assessed against a ground truth or a gold standard, providing an objective and transferable measure for the performance or efficacy of the approach. TOLIAS and PANAS (1998), HOOVER *et al.* (1998*b*; 2000) and SINTHANAYOTHIN *et al.* (1999) have produced the only studies, out of approximately 23 papers on vascular segmentation, to provide results describing the performance of the vessel segmentation algorithms.

Within these three studies, the definition of a true match varies. An exact match between pixels, corresponding to the same location in both images, was required by SINTHANAYOTHIN *et al.* (1999) and HOOVER *et al.* (2000). HOOVER *et al.* (1998*b*) only required neighbouring pixels to match. Vessel segments, defined as the tract of vessel between branching points, were used by TOLIAS and PANAS (1998). However, in this latter study, it was not clear how the correspondence between human- and algorithm-marked vessel segments was established.

The physical level or *a priori* knowledge of the retinal vessels is summarised in Table 1. Tracking or following the vascular arbour, its branches and convergences exploits *a priori* knowledge of the retinal vascular network.

Tracking saves computation time by avoiding scanning the entire image, whereas matched filters are swept over its entirety. In a similar way, neural networks are scanned over the whole image, the response of the filter or network being proportional to the likelihood of a vessel being present at one of the pixels of interest, usually the centre pixel.

For the purpose of this review, vascular segmentation is split into four separate areas: local operators, matched filters, vessel tracking and neural networks.

2.4.1 *Local vascular segmentation:*

The retinal vessels are darker than their surroundings, enabling segmentation of small regions by the use of a threshold. Pixel intensities above or below this threshold can be accepted as potentially belonging to a vessel, or discarded as background. Alternatively, pixel brightness values in a region can be homogenised. Areas of pixels can be clustered into groups, depending on their brightness and how they are connected to each other. This connectivity constraint determines the shape of the area and is usually called the structuring element. Grey-scale

Table 1 A priori knowledge of retinal vascular tree

Vessel	Feature	Description and reference
Segment	calibres	are invariant along their segment length; profiles are detailed by HAMMER *et al.* (1997) and RASSAM *et al.* (1994)
	curvature	vessel centrelines are regular, i.e. contain no discontinuities and have a finite range of rate of change of direction (HART *et al.*, 1997)
	length	is theorised to scale in a fixed ratio (WEST *et al.*, 1997)
	overlap	veins (arteries) do not overlap veins (arteries)
Branch	angle and number	branches from larger vessels to smaller ones are dichotomous and acute
	calibres	calibres of branches cannot be assumed to preserve volume, as blood slows down for metabolite transport
Special cases	twisted pairs	a rare helical arrangement of veins and arteries
	parenchymal dips	parts of segments are submerged within the opaque retina
	cilioretinal arteries	are small, arise from edge of OD and do not form part of whole vascular arbour

structuring elements have an intensity value that is added to the underlying image. If the result of the summation is larger than either the structuring element or the image, then it is kept. This process is repeated for all positions of the structuring element over the underlying image and is called dilation. If the structuring element is subtracted and the minimum value is kept, the process is called erosion. Noise and small artifacts can be removed in this way. Careful selection of regions enables local thresholding to work.

Studies assessing venous beading (KOZOUSEK *et al.*, 1992; GREGSON *et al.*, 1995) measure the variation in vascular calibre along a segment. Venous beading is assessed only in the larger vessels, where pixel intensity distributions are well separated from those of the retinal parenchyma. GREGSON *et al.* (1995) chose the regional threshold as equidistant from the means of background and vessel pixels, which in turn were defined as top and bottom cumulative percentiles; the percentage was not given. Erosion and dilation with a square-shaped operator after thresholding fill in gaps and remove bleeders. Precise estimation of the vessel edge is obtained by dividing the area under a vessel cross-section by the range of heights in its profile.

Some regions of the ocular fundus are devoid of major vessels, and methods, such as that of GREGSON *et al.* (1995), that use local dynamic thresholding fail and produce artifacts. AKITA and KUGA (1979) overcame this limitation by analysing groups of connected pixels. Multiple thresholds of the derivative image generate blobs, allowing area-based discrimination to discard components too small or large to be vessels.

YE and ZHENG (1995) used a spherical structuring element to enhance the difference between the fundus and background. To this image, thresholds over the full range of intensities were applied using the Otsu method (OTSU, 1979), where the final threshold satisfied max $[N_v N_f(\mu_v - \mu_f)^2]$, where N and μ were the number and mean intensity of vessel v and fundus f pixels, respectively.

The local gradient of the image, in the form of first and second directional derivatives, has also been exploited for vascular segmentation. YU *et al.* (1990), WANG and LEE (1997) and KATZ *et al.* (1988) used the first derivative, or Sobel operator, to find the magnitude and direction of the parallel edges of the vesels. They used the opposing and parallel gradients along the vessel to estimate the location of the vessel midline.

The second derivative, smoothed by a Gaussian of $\sigma = 4$, was investigated by MARTÍNEZ-PÉREZ *et al.* (1999*a*;*b*). They used the eigenvalues of the second derivatives of each pixel to obtain the maximum and minimum gradient, irrespective of their orientations. The Otsu method (OTSU, 1979) was then used to choose thresholds for the new distributions of pixel gradients after the eigenvalue transform. The means and standard deviations of the various classes obtained by these thresholds were then used to guide an iterated region growing procedure. The authors commented favourably on the applicability of this approach for images taken with the aid of contrast-enhancing agent and normal reflectance retinal photographs.

2.4.2 *Matched filters:* Matched filters are based upon similarity measures between an ideal signal and a measured signal. The sum of products of the translated matched filter over every point of the image is know as convolution and produces a probability image. A number of ideal signal profiles are available and are either based on assumptions about the anatomy and corresponding light transmittances or on empirical observation of actual vessel profiles. A number of parameters, such as length, width and orientation, describe the modelled profiles. Many other parameters are ignored; nevertheless, numerous potential matches need to be evaluated, making this approach computationally expensive in the absence of dedicated hardware.

The basic retinal vessel anatomy, represented by a circular or elliptical blood column coaxially surrounded by a thickness of wall material, has been used to generate cross-sectional profiles (RASSAM *et al.*, 1994; PATEL, 1995; HAMMER *et al.*, 1997). Other idealised profiles have been produced by the direct fitting or error minimisation of mathematical functions representing vessel profiles to the observed intensity profiles (ILIASOVA *et al.*, 1998; GAO *et al.*, 1997).

Usually, matched filters are two-dimensional cross-sections that are extruded or rotated into three dimensions. Extruded profiles are rotated to accommodate the varied orientations of the retinal vessels. Profiles that are rotated match any vessel orientation and need only to be convolved once at each image position. Matched filters that are only rotated are more susceptible to spurious detections (YANG *et al.*, 2000).

Retinal imaging varies in field of view and number of samples; parameters for the filters are thus resolution-dependent. For the extruded and rotated Gaussian filters, parameter selection has not differed from the original study (CHAUDHURI *et al.*, 1989*a*), with $\sigma = 2$ (GOLDBAUM *et al.*, 1989; 1993; GOH *et al.*, 1997; HOOVER *et al.*, 1998*b*; YANG *et al.*, 2000).

Other filter shapes have been investigated, including filters based on lines (WANG and LEE, 1997), partial Gaussians (CAN *et al.*, 1999), derivatives of Gaussians (POLI and VALLI, 1997) and ellipses (JASIOBEDSKI *et al.*, 1993). The first three of these filters consider computation time as an important design factor and rely upon binary or integer arithmetic taking less clock cycles than floating point calculations.

WANG and LEE (1997) apply filters that are $15\,\text{pixel}^2$, containing a line a single pixel wide, over 12 orientations. POLI and VALLI (1997) settled for a standard deviation of one, in their binomial approximation of a Gaussian. CAN *et al.* (1999) use two separate ranges of a Gaussian curve to create a matched filter corresponding to the flanks or skirts of a vascular profile.

By reducing the number of computer cycles per calculation and the total number of calculations, these studies have reduced computation time for vascular segmentation. Quantitative measures to characterise the performance of these studies are desirable, yet lacking. Matched filters do not work in isolation and form part of an algorithmic chain. They provide a non-binary measure of correlation that still needs classification into background or vessel. Thresholds divide the range of intensity of the filter response into two classes that are applied locally or globally.

HOOVER *et al.* (1998*b*) iteratively decrement the initial threshold (which is set to the matched filter response), so that a vessel blob is grown. This blob can be kept or discarded, depending on tests of size, relative position to already marked pixels and absolute threshold value.

Thresholds are applied to images that represent the intensity transitions of neighbouring pixels (YANG *et al.*, 2000). These image representations can be visualised as a two-dimensional array that has its number of rows and columns equal to the range of grey levels in the original image. The grey-level indices are used to accumulate the intensity transitions from each row number to column number for all neighbouring pixels in the original image.

The transformed image is useful because, when thresholded, it provides a tractable representation from which measurements can be taken to compare similarity. YANG *et al.* (2000) derived a threshold value that maximised the difference in this similarity measure and so started to segment the retinal vessels. The segmentation was finished after some of the smaller connected components (groups of pixels) were eliminated from the bilevel image.

Segmentation into vascular and non-vascular is necessary for comparison between studies or within studies to assess filter shape and parameter selection. HOOVER *et al.* (1998*b*) provided

the only evaluation against a human operator and reported a sensitivity (true positive fraction) of 80% and a specificity (true negative fraction) of 90% for a marked pixel matching any of its eight neighbours. The same performance was reported in a later paper (HOOVER *et al.*, 2000), presumably for a one-to-one correspondence between human-marked and computer-processed pixels.

2.4.3 *Vascular profile tracking:* From a start point on a vessel, profile tracking iteratively scans for, selects and follows pixels belonging to the retinal vascular arbour. The selection of vascular points is accomplished using two- or three-dimensional matched filters. Fuzzy vessel profile recognition and intensity based algorithms provide alternatives to matched filtering (TOLIAS and PANAS, 1998; WANG *et al.*, 1990).

The two-dimensional profile tracking algorithms reviewed used Gaussian, or a derivative of Gaussian, filters. Profiles are available that represent the vascular cross-section with less divergence in width (RASSAM *et al.*, 1994); however, these are not as analytically simple to allow least square fitting (FRAME *et al.*, 1997*a*) or for deriving indices (TAMURA *et al.*, 1988; ZHOU *et al.*, 1994) to define vessel edge and thus width.

The profiles used are only apt for describing single vessel segments, but vasculature branches and arterio-venous crossings are common. This presents a special case for tracking. FRAME *et al.* (1997*a*) used a measure of profile skewness to create new starting points for the algorithm. In a similar fashion, TAMURA *et al.* (1988) used vessel width ranges to trigger sampling of a relatively large and circular cross-sectional profile to which the filter is applied. The number of responses indicates whether branching, crossing or a vessel end point has occurred. CAN *et al.* (1999) used an asymmetry measure of the template response to trigger new tracking. KOCHNER *et al.* (1998) prospectively scanned alongside, or parallel to, the vessels that were segmented during the the first pass to detect branchings or crossings.

2.4.4 *Artificial neural network vascular segmentation:* The operation of a neural network is analogous to that of a matched filter. Both take subwindows of the image as input and return a probability measure as output. Two studies, both using the back-propagation algorithm, have detected (GARDNER *et al.*, 1996) and segmented (SINTHANAYOTHIN *et al.*, 1999) the retinal vasculature. Detection entailed classifying subwindows as containing vessels or not; segmentation classified individual pixels.

Neural networks require training examples; these examples were created by a human operator. Sinthanayothin *et al.* used 25 094 labelled (pixel-by-pixel) examples, each of 200 pixels in area. However, it was not clear whether they labelled ≈ 2.5 million pixels to create independent and non-overlapping examples, or whether they labelled an area that could generate 25 094 examples whose input (but not output) areas overlapped.

The neural networks researched by GARDNER *et al.* (1996) used 20×20 pixel subwindows. Nine thousand of these subwindows were marked for neural learning validation. Generalisation assessment over 1200 unseen subwindows resulted in a sensitivity and specificity of 91.7%. SINTHANAYOTHIN *et al.* (1999) achieved a sensitivity of 83% and a specificity of 91% in classifying pixels.

3 Image processing for diabetic retinal pathology

The grading methods of the early treatment diabetic retinopathy study (ETDRS) described the assessment of at least 22 categories of lesions with respect to DR (ETDRS RESEARCH GROUP, 1991*a*). There are other, less formal, grading concepts used in DR assessment, adding to the number of lesion categories. Grading concepts, such as ischaemia and 'dots and blots', have not been assessed in the early treatment trials for prognostic significance.

When this variation is combined with the natural variability of the image and the variety of confounding non-diabetic pathologies, it makes segmenting lesions a difficult task (DONOHOE *et al.*, 1999). Research has focused on the identification of exudates, micro-aneurysms and haemorrhages, which are relatively numerous and easier to define in terms of area and perimeter.

3.1 *Registration of retinal images*

If screening incorporates digital imaging of the retina, multiple images are usually recorded for each eye at examinations. The magnification and location of each image differ. In systematic screening, the locations of these images on the retina, as well as the field of view, are defined by the screening protocol, and variability in these protocols is compensated for by the human interpreter.

Digital analysis, in an analogous fashion to human interpretation, seeks to standardise the retinal areas of interpretation. Registration, or finding a single spatial and temporal co-ordinate set, enables the repeatable analysis of exactly the same scene or domain in different fundus images of the same eye. Registration can thus monitor changes and differences in a given area of retina and also enables integration of images to cancel noise or to create wide-angle image montages.

The unknown geometric distortion arising from the lens and the spherical nature of the retina introduce some non-linear distortions. However, the assumption of a planar area of interest, combined with relaxed requirements for the fidelity of the geometrical transform, enables rotation, scaling and translation (RST) distortions to be modelled.

Many methods have been proposed for registration, but a demonstration of their potential for automated registration outside laboratory conditions remains (WOOD, 1990; GOH *et al.*, 1997; RYAN and HENEGHAN, 1999). The difference between precisely registered serial images was used as an indicator of developed non-diabetic pathology by CIDECIYAN *et al.* (1992) and GOLDBAUM *et al.* (1993). However, no studies have been found expanding upon this methodology.

BALLERINI (1998) presents a method to compensate for motion and the changes in contrast resulting from the fluorescent dye travelling down the retinal and subretinal vasculature. This could have applicability in imaging modalities for screening, where annular or crescent-shaped areas of low contrast move from image to image.

Other registration tasks have been developed for motion compensation or tracking. DOMINGO *et al.* (1997) investigated motion recovery in variable-contrast angiograms of the retina. Albeit not directly applicable to screening, investigations managing and incorporating variable and 'badly behaved' marker points into algorithms for the estimation of the geometrical transform are useful. They are useful because a significant proportion of each retinal image is irregular, owing to previous therapy, non-diabetic pathology or to factors (described in Section 2.2) intrinsic to the imaging process. Real-time systems used to locate, guide and verify the placement of the laser for photocoagulation of the retina may one day be incorporated into image acquisition systems for screening. Details of the algorithms and performance characteristics are given in Table 2.

3.2 *Micro-aneurysm segmentation*

Micro-aneurysms are spherical balloonings of the vascular wall; their segmentation is based upon elimination of linear

Table 2 Overview of registration approaches

Study	Transform	Error	Markers	Summary of algorithm
GOLDBAUM *et al.* (1993)	RST	registration failed in 16%	matched filter response	correlation of POI to form feature pairs; iterative least squares on decreasing best-fit percentiles
SPENCER *et al.* (1996)	non-linear	NA	human-marked anatomy	VisiLog
GOH *et al.* (1997)	translation	nine image montage accrued errors of 5 pixels	whole image	error-threshold-restricted global search by translation of images
RYAN and HENEGHAN (1999)	RST	sum squared of intensity difference was 1%	human-marked anatomy	POI pairs form vectors; metrics describing tentative R, S and T transforms for all vector pairs between images are plotted; largest cluster is taken as correct transform
DOMINGO *et al.* (1997)	RST	MSE 0.84–16.6 pixels. Failed in five out of 52 owing to POI selector	POIs selected by Förstner's operator	approximation of correspondence pairs based on Euclidian distance between feature vectors; followed by either iterative refinement or a least squares error by discarding points furthest from match
TANAKA and TANAKA (1988)	translation	NA	vessel branching points	correlation between features of branching points (length and direction of branches); matching points are plotted on a scatter diagram; largest clusters are taken to represent translation
BALLERINI (1998)	translation	NA	matched filter response	cross-correlation of binary images.
BECKER *et al.* (1998)	translation and scaling	average 1.35 pixels, always below 4 pixels	points of edge direction dispersion	disperion measure of edge strength-direction histogram is used to reject candidate points; best five matches start clustering for remaining points; candidate transform is validated using an empirically set normalised sum-of-differences between images and minimised via least squares
BARRETT *et al.* (1994)	translation	NA	vessel cross-section templates	small templates are scanned over a constrained area derived from maximum theoretical displacements
CIDECIYAN *et al.* (1992)	RST	average pixel intensity SD = 4.65	whole image	log-polar representation of image, in Fourier domain, allows scaling and rotation to be represented as shifts that are amonable to a 'brute force' cross-correlation approach

MSE = mean squared error; NA = none available; POI = points of interest; RST = rotation scale translation

structures and subsequent feature-based discrimination of candidate areas. Exudates, which are lipid-like deposits, are segmented by thresholding in alternate colour spaces. Texture information is used to classify larger regions of pathology, such as new vessel growth and ischaemia. The fractal dimension, representing the degree to which the structure fills the dimensions in which it is embedded, is also used to study new vessel growth.

Micro-aneurysms range in size between 12μm and 125μm. The small size of micro-aneurysms means that image processing is usually applied to images obtained with the aid of a blood-borne contrast agent. However, these methods and techniques have also been applied, with some success, to conventional reflectance images.

Micro-aneurysm segmentation usually started with the subtraction of an image containing linear features. These features were detected by erosion and subsequent dilation with a linear structuring element (PHILLIPS *et al.*, 1991; SPENCER *et al.*, 1994; 1996; FRAME *et al.*, 1996; CREE *et al.*, 1997; MENDONÇA *et al.*, 1999). The resulting image was match filtered (using an 11×11 pixel 2D Gaussian filter of $\sigma = 1$) and thresholded to obtain seed points. Pixels were added to the seed-points to form regions, the inclusion criteria being based upon an empirical contrast ratio between the background and the intensity of the seed pixel. Parameters such as area, perimeter and energy (sum of squared intensities) were used to described each region.

Humanly delineated micro-aneurysms enabled decision boundaries to be drawn on distribution plots of these parameters; segregating the candidate regions into presumed micro-aneurysm and spurious artifact. SPENCER *et al.* (1996) achieved a sensitivity of 82% at a cost of detecting between 100 and 150 false positives over four images. CREE *et al.* (1997) improved on this by using more parameters and reduced the false positive rate to 5.7 per image for the same sensitivity. A sensitivity of 66% was achieved by EGE *et al.* (1998), with 107 false positives from a sample containing 316 micro-aneurysms.

3.3 *Exudate and haemorrhage segmentation*

Exudates, like micro-aneurysms, are an early indicator of diabetic retinal disease. Human selection of the yellow and waxy sheened pixels representative of exudate areas was used to plot scattergrams of colour features of these pixels (GOLDBAUM *et al.*, 1990*b*). More specifically; a brightness-independent representation of exudate colour was plotted with the same representation of haemorrhage and infarct lesions. Boundaries set by human operators distinguished the three types of lesion on these

scattergrams. The system was only tested to classify pixels that had already been selected by a human. Exudates were thus distinguished from other focal lesions in seven out of ten cases.

WARD *et al.* (1988) presented an empirical and interactive global technique for thresholding a noise-reduced (mean-filtered, 64 pixel^2) image to segment exudates. A fully automated method applied a 'simple threshold' after the vessels and OD had been removed (KOCHNER *et al.*, 1997). 'Simple thresholding' was also used by ZAHLMANN *et al.* (2000) and was based upon an initial threshold value that segmented 5% of the brightest pixels. This was used to probe, under empirical area constraints, for more exudate pixels. The edge responses of the potential exudative pixels and their surrounding neighbourhood provided further basis for discrimination.

EGE *et al.* (1998) detected all but ten of 390 exudative lesions to give a sensitivity of 97%; no details were given of the algorithm. In a later paper (EGE *et al.*, 2000), a region-growing approach was used upon seed points derived from a background-subtracted image. A median filter, 31 pixel^2, allowed thresholds to be set to segment partially bright lessions such as exudates. An empirically constrained region-growing algorithm then further segmented the candidate areas. Features extracted from this region were assessed for significance and presented to three classification methods. A nearest neighbour-based classification was able to discern all exudates (100% sensitivity) in 134 images.

HUNTER *et al.* (2000) evaluated abstract features derived from statistics and transforms summarising subwindows of the image. From a data set of 16 images, 211 subwindows, each 16 pixel^2, were found and marked as containing exudates or drusen (which are similar to exudates, but are more recessed and punctuate in appearance). For each of these subwindows, 178 features were developed and were based on the raw image, the Fourier transform and the directional derivatives. From these 178 features, it was found that an input feature vector of 11 data points was necessary to achieve a sensitivity and specificity of 91% in the detection of these lesions.

Texture-based segmentation was applied by FRAME *et al.* (1997*b*): exudates were marked by a human, and their intensity histogram and their spatially dependent intensity transition (an indicator of texture) probabilities were computed. A Gaussian form was assumed for the distribution of metrics describing the exudates and normal background. Prospective exudate pixels were classified according to the distance from the mean of the humanly marked ones. Classification performance was described as inferior to that of interactive global thresholding.

Haemorrhages have irregular boundaries and are either flame- or feather-like in texture and shape. They range in size from relatively extensive (occupying quartiles of an image) to small and approaching the size of micro-aneurysms. LEE *et al.* (1999) used sequential or staggered global thresholding and a sampling grid formed from the intersection of radial lines and concentric circles converging to the macula for segmentation. They described their results as 'manually verified and found in good agreement with the manual counts'.

Haemorrhage detection by EGE *et al.* (1998) was successful in 140 out of 155 lesions. Neural networks have also been applied to the detection of haemorrhages. More than 12 000 subwindows (30 pixel^2) were used to train and test a back-propagation network that achieved a sensitivity and specificity generalisation ability of 73.8% (GARDNER *et al.*, 1996).

BERRY and WESTERMAN (1998) proposed a clustering algorithm for the identification of micro-aneurysms, haemorrhages and the vasculature. The assignment of a lesion type to the clusters was based on the major and minor axes of the bounding ellipse and an intensity-modulated measure of spread, termed the radius of gyration. These metrics seemed to vary with lesion type but were not integrated or applied to the segmentation of haemorrhages. A similar approach was proposed by LEE and WANG (1998), where a range of thresholds provided binary images for various matched filters corresponding either to vessels or punctuate or diffuse lesions.

3.4 *Analysis of the ischaemic and neovascular retina*

The capillaries of the retina help determine the texture and appearance of the fundus. The presence of new vessels is associated with a high risk of progression to the sight-threatening stages of diabetic retinopathy. Likewise, atrophy of the normal capillary bed, causing ischaemia, indicates progression at an earlier stage of pathology. The border of the capillary bed surrounding the area of greatest visual acuity is mildly curved in shape; disturbances in this boundary region indicate changes in the distribution of the capillary bed.

JASIOBEDSKI *et al.* (1993), working with contrast-enhanced retinal images, compared an ischaemic classification algorithm with classifications by an ophthalmologist. Their segmentation approach was singular in that pixels were amalgamated into homogenous regions. These were created by smoothing, erosion followed by dilation and a reduction in the number of grey levels. From the resulting patchwork or tessellation of regions and their borders, the vessels were detected by matched filtering (with a semi-elliptical profile) normal to the borders. This enabled vessel pixels to be excluded from metrics describing the region's interior texture. The change in intensity in the patches that occurred with different structuring elements used in the erosion and dilation described the abundance and extent of features within that region. The system reached a specificity and sensitivity of approximately 80% compared with the classifications given by an ophthalmologist.

Ischaemia can lead to new vessel growth and changes to the avascular zone of the fovea. FRAME *et al.* (1997*b*) used the intensity histogram to derive texture metrics for neovascular areas. Regions with and without neovascularisation were selected and marked by humans and provided a training set to optimise the weights for the classifier (linear discriminant analysis). The human-marked classes were linearly separable, but applicability to new data was found to be disappointing.

The fractal dimension of a retinal region gives a scale-invariant description of how features fill that region. Measures of the fractal dimension have been applied to study patterns of neovascularisation. Although not true fractals (PANICO and STERLING, 1995; WEST *et al.*, 1997) and better described as space filling, vessel segment lengths are clearly disturbed during neovascularsation.

The fractal dimension, as measured in a region of interest (ROI) using the density–density correlation method, has been shown to change for a patient over the course of neovascularisation (DAXER, 1993*a*) and between normal and neovascularised retinae (DAXER, 1993*b*). LANDINI *et al.* (1993) measured the fractal dimension for whole retinal images of normal retinas and for those with venous oclusion (LANDINI *et al.*, 1995) and found no difference. However, the fractal dimension of connected components within subwindows distinguishes pathological and normal states. Unfortunately, the fractal studies segmented the retinal vasculature by manually tracing the vessel midlines on paper and so lost their applicability for automation.

The rounded transition zone from vascular to avascular retina surrounding the foveola has been delineated with contours fitted using genetic algorithms. Parameters describing the flexibility and length of the contour were tweaked (BALLERINI, 1999). The position and shape of the contour were then found within a pre-centred annular area on the fovea by mutating, recombining and selecting the best solutions over many generations of trials. Two sample contours were presented.

4 Intelligent systems for DR analysis, diagnosis and screening

A modular intelligent system for DR diagnosis would identify and segment each type of lesion; so that, by reference to a grading scheme, the level of DR could be ascertained. In practice, once some pathology has been segmented, attempts are made to use that information. For example, the absence or questionable presence of micro-aneurysms would not require immediate intervention. Exudates and haemorrhages have also been used to provide information for diabetic ocular health care.

GARDNER *et al.* (1996) used a neural network to classify subwindows as vessel, haemorrhage or exudate. With this information, the system was compared with the referral rates of an ophthalmologist. The Gardner *et al.* system would not have missed any patient that required referral (99% sensitive) and was 69% specific; in other words, 31% of all diabetics not requiring attention would have been flagged for referral. No details were given on how the information on exudates and haemorrhages was encoded and integrated to come to this decision.

ALEYNIKOV and MICHELI-TZANAKUO (1998) described a neural system with input features based on the spatial frequencies present within a sub-image. They also used various averages of these subwindows to form the inputs to a neural network that had targets derived from a human classification of the severity of haemorrhages. System performance was poorly specified; the reported accuracy of 79% does not give information on the classification of true negatives and true positives for a given prevalence.

HIPWELL *et al.* (2000) evaluated an intelligent system for screening DR. A human grader classed 3783 images with reference to standard photographs, according to the EURDIAB protocol (ALDINGTON *et al.*, 1995). Three aspects of this grading scale were compared with the micro-aneurysm detector (SPENCER *et al.*, 1996; CREE *et al.*, 1997) described in Section 3.2. The micro-aneurysm segmentation algorithm, operating as an intelligent screening tool, was set to give a positive result if any micro-aneurysm was detected. A comparison with the human grader is summarised in Table 3. This system could reject 76% of all patients with no DR at the expense of rejecting 15% of patients who actually have DR (according to the grading methodology and criteria used).

HIPWELL *et al.* (2000) demonstrated how, for a given grading methodology, screening based upon segmentation of a single feature can save diabetic health care resources. ZAHLMANN *et al.* (2000) proposed an elaborate system that encompassed some of the non-imaging aspects of DR grading and screening. Inputs describing the patients' metabolic profile, treatment history and visual acuity were combined with parameters from retinal image segmentation. The vascular arbour (segmented as in KOCHNER *et al.* (1998)) was obtained and was used as a framework from which to identify the OD and foveal area, but it was not used *per se* in subsequent intelligent analyses. The exudative area, described in Section 3.3, and all the other inputs were given a degree of significance by a medical expert. Fuzzy rules, tuned using simulated data, were tested upon 12 real patient data sets, eight of which had retinopathy not detectable using non-stereoscopic retinography alone i.e. macular oedema. The system classified correctly 96% of image-based decisions and 76% of cases partially involving non-photographic data. No break-down was given of the type of truth (true positives or true negatives) for which the system was correct.

There have been many other abstracts and poster presentations on automated screening for DR. Implementation details and performance results are less detailed than those reviewed in this Section. Table 4 summarises their approaches and claims.

Table 3 Prospective validation of micro-aneurysm detection for DR screening with 3783 images or 925 studies. 174 images were classified by human grader into questionable category for micro-aneurysm present; these were not comparable with output from micro-aneurysm detection algorithm. All data are from HIPWELL et al. (2000)

	Single image		Complete study
	Micro-aneurysms (number of cases detected)	DR (number of cases detected)	DR (number of cases detected)
Sensitivity, %	81 (736 913)	78 (745 956)	85 (315 372)
Specificity, %	93 (2 502 2696)	91 (2 576 2827)	76 (423 553)

Table 4 Communications presenting intelligent systems for DR analysis

Study	Methods	Presented outcome
ZAHLMANN *et al.* (1996)	no details	proposal of interactive, on-line DR atlas and diagnostic query tool
NGUYEN *et al.* (1996)	neural classification of segmented lesions	human-labelled images compressed and automatically graded according to ETDRS RESEARCH GROUP (1991*a*) using back-propagation neural networks
CASI *et al.* (1996)	fuzzy neural	graphical user interface to ease access to HIS, PACS and intelligent diagnostic modules
SINCLAIR *et al.* (1996)	no details	automated classification (conforming to early version of ETDRS RESEARCH GROUP (1991*a*)) claimed to compare well with that of retinal specialist; third grading standard is implied but not specified
GOLDBAUM *et al.* (1996)	no details	database of images is presented that can be queried by lesion type and thus retinopathy grade; querying mechanism works upon automatically generated index
THOMPSON (1999)	neural analysis of wavelet-compressed images	images from 150 subjects (256 × 256 pixels) reduced to 176 orthogonal wavelet coefficients; neural classification of coefficients was 83% specific and sensitive
DONOHOE *et al.* (1998)	neural analysis with interactive segmentation of lesions	neural labelling of lesions guided by human operator enables semi-quantitative labelling of fundus areas

5 Summary and discussion

Owing to the scarcity of objective results, only a few of the studies reviewed are worthy of note. For anatomical image-analysis, neural- and variance-based algorithms for the segmentation of the vasculature and OD have effective performance (SINTHANAYOTHIN *et al.*, 1999). The vascular segmentation results of HOOVER *et al.* (2000) are remarkable for the use of a representative data set and may be more relevant and reliable with respect to screening situations. In these non-ideal environments, image quality, previous therapy and non-diabetic lesions will interfere with analysis unless these images are pre-emptively flagged, as suggested by LEE and WANG (1999).

The intelligent system proposed by HIPWELL *et al.* (2000) demonstrated that diabetic patients can be reliably dichotomised into those with definitely no micro-aneurysms and those with possible micro-aneurysms. This was achieved by empirical means, whereby the properties of human-labelled micro-aneurysms could be plotted with candidate areas produced by the algorithm. In this feature, space decision boundaries could be drawn. Screening on the basis of establishing the absence of micro-aneurysms is an important first step, but it does not reliably identify the diabetic patient with no DR.

The image types, patient information and lesions required for medical management decisions for DR are well-defined, clearly demonstrated and well-disseminated. It is clear that digital imaging can only record a subset of this data. To compare results of lesion or anatomy segmentation for intelligent decisions or otherwise, a defined standard needs to be referenced. Pre-selection of the test images, local standards for DR grading and qualitative description of results do not allow objective comparisons but are common in the literature (GOLDBAUM *et al.*, 1989; CASI *et al.*, 1996; NGUYEN *et al.*, 1996; ZAHLMANN *et al.*, 1996; 2000; ALEYNIKOV and MICHELI-TZANAKUO, 1998; BERRY and WESTERMAN, 1998).

The gold-standard method for grading and describing DR is seven-field stereoscopic photography. This is a descriptive and labour-intensive grading protocol that enables effective timing and early treatment to prevent or delay sight loss (DRS RESEARCH GROUP, 1987; ETDRS RESEARCH GROUP, 1985; 1991*b*).

Novel grading schemes are validated against this grading method (KLEIN *et al.*, 1986; ALDINGTON *et al.*, 1995), and epidemiological studies use the detail it provides to monitor incidence and the effects of therapy (KLEIN *et al.*, 1989; DCCT RESEARCH GROUP, 1995). There are thus a well-established diagnostic framework and objective criteria by which pathology segmentation algorithms or intelligent systems can be evaluated.

However, there is still debate as to whether digital imaging is capable of capturing enough, or all, of the required information. The aspect of DR know as macular oedema can only be detected if stercoscopic images are taken or by direct examination, such as slit-lamp biomicroscopy. The detection of drusen is also aided by stereopsis. AIELLO *et al.* (1998*b*) took stereopsis into account when assessing digital imaging for DR diagnosis. The study found that 30° stereoscopic grading of DR using digital images according to the ETDRS protocol was feasible.

Non-stereoscopic digital-imaging screening has also been favourably proposed (YOUNG *et al.*, 1997; GEORGE *et al.*, 1997; LIESENFELD *et al.*, 2000; HENRICSSON *et al.*, 2000). The lower resolution of digital images compared with that of photographic film was not found to hamper stereoscopic DR diagnosis and the detection of drusen (AIELLO *et al.*, 1998*b*; SOLIZ *et al.*, 2000). Topographic images digitally representing the baseline disparity have been proposed by BERESTOV (2000) and hold great potential for the analysis of macular oedema.

The inclusion of macular oedema into automated screening is important and relevant, because a significant proportion, $\approx 10\%$ (KLEIN *et al.*, 1989), of sight-threatening cases would be missed by the segmentation techniques and developing intelligent screening systems reviewed in this paper, even at a sensitivity of 100%. It is precisely for patients with macular oedema that early treatment is indicated, because it is for these patients that sight loss can be prevented as opposed to halted (ETDRS RESEARCH GROUP, 1985).

Image analysis is starting to address the constraints and implications found in the underlying data generation mechanisms found in actual diabetic screening. HOOVER *et al.* (2000) and LEE and WANG (1999) have integrated problems that would badly affect most of the algorithms presented. Issues such as non-diabetic lesions, previous treatment and different imaging protocols are all still confounding factors. Image quality has also been identified as a limiting factor (HIPWELL *et al.*, 2000; EGE *et al.*, 2000).

The few research papers investigating full automation for screening emphasise that detection of pathology should trigger further referral; high sensitivities are required to ensure false negatives do not occur, and this approach lightens the burden on screening personnel by flagging abnormal images. Inverting the screening task, i.e. detecting normal diabetic retinae, would accomplish the same result, releasing safe patients back into the screening pool and flagging suspect cases of all pathology types.

The concerns regarding the subjective reporting of results are aptly put forward by PELI (1993), who highlights the need for the objective evaluation of the efficacy of systems. Although Peli discusses image enhancement, the lack of validity in transferring evidence of improved performance in the laboratory to a clinical situation needs careful consideration within automated screening as well, as it has been found that computer systems aiding in the diagnosis are not as effective as simple and objective interpretative aids, such as formal protocols and reference diagrams. This improvement has also been borne out in studies for the automation of diagnosis of pulmonary embolisms (FISHER *et al.*, 1996; SCOTT *et al.*, 1996).

Further parallels between screening for pulmonary embolisms, cardiac infarcts and DR are notable. Many intermediary representations or features that have no analogue in modular, or lesion-by-lesion, grading can be exploited for DR analysis. BAXT (1994), BAXT and SKORA (1996) and the aforementioned pulmonary embolism studies echo the work of HUNTER *et al.* (2000) and ALEYNIKOV and MICHELI-TZANAKUO (1998) on the use of unconventional prognosticators of disease. However, the analysis of the significance of single features by HUNTER *et al.* (2000) is likely to ignore the non-linear interactions so fruitfully exploited by BAXT and SKORA (1996).

One of the more promising indices of DR is described by KRISTINSSON *et al.* (1997), who have uncovered an interesting correlation between vascular segment length and developing macular oedema. The algorithms presented by GREGSON *et al.* (1995); KOCHNER *et al.* (1998); HOOVER *et al.* (2000) and SINTHANAYOTHIN *et al.* (1999) are well positioned, with a little modification, to extract segment length and calibre information and so include the diabetic population for which the timing of the detection and treatment of asymptomatic DR lesions is so critical.

Acknowledgments—The retinal image in Fig. 1 was provided courtesy of the ETDRS and DRS Research Groups.

References

AIELLO, L., CAVALLERANO, J., GARDNER, T., KING, G., BLANKENSHIP, G., FERRIS, F., and KLEIN, R. (1998*a*): 'Diabetic retinopathy', *Diabetes Care*, **21**, pp. 143–156

AIELLO, L., BURSELL, S., CAVALLERANO, J., KELLY GARDNER, W., and STRONG, J. (1998*b*): 'Joslin vision network validation study: Pilot image stabilization phase', *J. Am. Optometr. Assoc.*, **69**, pp. 699–710

AKITA, K., and KUGA, H. (1979): 'Towards understanding color ocular fundus images'. *Proc. 6th IJCAI*, Tokyo, Japan, pp. 7–12

AKITA, K., and KUGA, H. (1982): 'A computer method of understanding ocular fundus images', *Pattern Recognit.*, **16**, pp. 431–443

ALDINGTON, S., KOHNER, E., MEUER, S., KLEIN, R., and SJOLE, A. (1995): 'Methodology for retinal photography and assessment of diabetic retinopathy: the EURODIAB IDDM complications study', *Diabetologia*, **38**, pp. 437–444

ALEYNIKOV, S., and MICHELI-TZANAKUO, E. (1998): 'Classfication of retinal damage by a neural network based system', *J. Med. Syst.*, **22**, pp. 129–136

AMERICAN DIABETES ASSOCIATION (1999): 'American diabetes association: Clinical practice recomendations 1999'. Technical Report S1, American Diabetes Association

BALLERINI, L. (1998): 'Integration of retinal image sequences'. Proceedings of SPIE Conference on Applications of Digital Image Processing XXI, **3460**, pp. 237–248

BALLERINI, L. (1999): 'Detection and quantification of diabetic retinopathy'. Proceedings of SPIE Conference on Applications of Digital Image Processing XXII, **3808**, pp. 213–223

BARRETT, S., JERATH, M., RYLANDER III, H., and WELCH, A. (1994): 'Digital tracking and control of retinal images', *Optical Eng.*, **33**, pp. 150–159

BAXT, W. G. (1994): 'A neural network trained to identify the presence of myocardial infarction bases some decisions on clinical associations that differ from accepted clinical teaching', *Med. Decis. Making*, **14**, pp. 217–222

BAXT, W. G., and SKORA, J. (1996): 'Prospective validation of artificial neural network trained to identify acute myocardial infarction [see comments]', *Lancet*, **347**, pp. 12–15

BECKER, D., CAN, A., TURNER, J., TANNENBAUM, H., and ROYSAM, B. (1998): 'Image processing algorithms for retinal montage synthesis, mapping, and real-time location determination', *IEEE Trans. Biomedical Eng.*, **45**, pp. 105–117

BERESTOV, A. (2000): 'Stereo fundus photography: automatic evaluation of retinal topography'. Proceedings of SPIE Conference on Stereoscopic Displays and Virtual Reality Systems VII', pp. 50–59

BERRY, M., and WESTERMAN, D. (1998): 'Cluster form analysis techniques for diabetic retinopathy', *Proc. Math. Models Med. Health Sci.*, pp. 35–50

CAN, A., SHEN, H., TURNER, J., TANENBAUM, H., and ROYSAM, B. (1999): 'Rapid automated tracing and feature extraction from retinal fundus images using direct exploratory algorithms', *IEEE Trans. Inform. Technol. Biomed.*, **3**, pp. 125–138

CASI, E., CERAVOLA, A., CIONINI, R., SPERDUTI, A., STARITA, A., and VITI, S. (1996): 'Diabetic retina analyser' in BOOM, H. (Ed).: 'Proceedings of 18th Annual International Conference of IEEE Engineering in Medicine and Biology Society' (Amsterdam, The Netherlands), pp. 1128–1129

CHAUDHURI, S., CHATTERJEE, S., KATZ, N., NELSON, M., and GOLDBAUM, M. (1989*a*): 'Detection of blood vessels in retinal images using two-dimensional matched filters', *IEEE Trans. Med. Imag.*, **8**, pp. 263–269

CHAUDHURI, S., CHATTERJEE, S., KATZ, N., and GOLDBAUM, M. (1989*b*): 'Automatic detection of the optic nerve in retinal images'. IEEE International Conference on Image Processing, Singapore, Vol. 1, pp. 1–5

CIDECIYAN, A., JACOBSON, S., KEMP, C., KNIGHTON, R., and NAGEL, J. (1992): 'Registration of high resolution images of the retina', Proceedings of SPIE Conference on Medical Imaging VI: Image Processing, **1652**, pp. 310–322

CREE, M., OLSON, J., MCHARDY, K., SHARP, P., and FORRESTER, J. (1997): 'A fully automated comparitive microaneurism digital detection system', *Eye*, **11**, pp. 622–628

DASBACH, E., FRYBACK, D., NEWCOMB, P., KLEIN, R., and KLEIN, B. (1991): 'Cost-effectiveness of strategies for detecting diabetic retinopathy', *Med. Care*, **29**, pp. 20–39

DAXER, A. (1993*a*): 'Characterization of the neovascularisation process in diabetic retinopathy by means of fractal geometry: diagnostic implications', *Graefe's Arch. Clin. Exp. Ophthalmol.*, **231**, pp. 681–686

DAXER, A. (1993*b*): 'The fractal geometry of proliferative diabetic retinopathy: implications for the diagnosis and the process of retinal vasculogenesis', *Current Eye Res.*, **12**, pp. 1103–1109

DCCT RESEARCH GROUP (1995): 'Progression of retinopathy with intensive versus conventional treatment in the Diabetes Control and Complications Trial', *Ophthalmology*, **102**, pp. 647–661

DIABETES UK (2000): '*Diabetes in the UK—the missing million*'. The British Diabetes Association

DOMINGO, J., AYALA, G., SIMO, A., DEVES, E., MARTINEZ COSTA, L., and MARCO, P. (1997): 'Irregular motion recovery in fluorescein angiograms', *Pattern Recognit. Lett.*, **18**, pp. 805–821

DONOHOE, G., SOLIZ, P., and NEMETH, S. (1998): 'Computer-aided image analysis for background diabetic retinopathy'. Proceedings of SPIE Conference on Medical Imaging 1998: Image Processing, **3338**, pp. 1017–1027

DONOHOE, G., NEMETH, S., and SOLIZ, P. (1999): 'An interactive system for computer-aided retinal image analysis'. 12th IEEE Symposium on Computer Based Medical Systems, 306, Los Alamitos, pp. 184–189

DRS RESEARCH GROUP (1981): 'Report 7. a modification of the airlie house classification of diabetic retinopathy', *Invest. Opthalmol. Vis. Sci.*, **21**, pp. 210–226

DRS RESEARCH GROUP (1987): 'Indications for photocoagulation treatment of diabetic retinopathy: Diabetic retinopathy study report number 14', **27**, pp. 239–253

EGE, B., HEJLESEN, O., LARSEN, O., JENNINGS, B., KERR, D., and CAVAN, D. (1998): 'Screening for diabetic retinopathy using computer based image analysis and bayesian classification', *Diabetes, Nutrit. Metabol.*, **11**, p. 95

EGE, B., HEJLESEN, O., LARSEN, O. V., M, JENNINGS, B., KERR, D., and CAVAN, D. (2000): 'Screening for diabetic retinopathy using computer based image analysis and statistical classification', *Comput. Methods Progr. Biomed.*, **62**, pp. 165–175

ETDRS RESEARCH GROUP (1985): 'Photocoagulation for diabetic macular edema: Early treatment diabetic retinopathy study report number 1', *Arch. Ophthalmol.*, **103**, pp. 1796–1806

ETDRS RESEARCH GROUP (1991*a*): 'Grading diabetic retinopathy from stereoscopic color fundus photographs- an extension of the modified Airlie House classification: Early treatment diabetic retinopathy study report number 10', *Ophthalmology*, **98**, pp. 786–806

ETDRS RESEARCH GROUP (1991*b*): 'Early photocoagulation for diabetic retinopathy: Early treatment diabetic retinopathy study report number 9', *Ophthalmology*, **98**, pp. 766–785

FISHER, R., SCOTT, J., and PALMER, E. (1996): 'Neural networks in ventilation-perfusion imaging; part 1. Effects of interpretive criteria and network architecture', *Radiology*, **198**, pp. 699–706

FRAME, A., CREE, M., OLSON, J., UNDRILL, P., MCHARDY, K., SHARP, P., and FORRESTER, J. (1996): 'Computer based classification of retinal micro-aneurysms'. International Conference on Neural Networks and Expert Systems in Medicine and Health Care, Plymouth, United Kingdom, pp. 50–56

FRAME, A., UNDRILL, P., OLSON, J., MCHARDY, K., SHARP, P., and FORRESTER, J. (1997*a*): 'Structural analysis of retinal vessels'. Proceedings of 6th International Conference on Image Processing and its Applications, IEE, Dublin, Vol. 2, pp. 824–827

FRAME, A., UNDRILL, P., OLSON, J., MCHARDY, K., SHARP, P., and FORRESTER, J. (1997*b*): 'Texture analysis of retinal neovascularisation'. Proceedings of IEE Colloquium on Pattern Recognition, London, Vol. 6, pp. 1–6

GAO, X., BHARATH, A. A., HUGHES, A., A., S., CHAPMAN, N., and THOM, S. (1997): 'Towards retinal vessel parameterisation'. Proceedings of SPIE Conference on Medical Imaging, **3034**, pp. 734–744

GARDNER, G., KEATING, D., WILLIAMSON, T., and ELLIOT, A. (1996): 'Automatic detection of diabetic retinopathy using an artificial neural network: a screening tool', *Br. J. Ophthalmol.*, **80**, pp. 940–944

GEORGE, L., LEVERTON, C., YOUNG, S., LUSTY, J., DUNSTAN, F., and OWENS, D. (1997): 'Can digitised colour 35 mm transparencies be used to diagnose diabetic retinopathy?', *Diabet. Med.*, **14**, pp. 970–973

GOH, K., SARKODIE-GYAN, T., CAMPBELL, A., SIMPSON, D., and MCNEELA, B. (1997): 'Computer assisted photocoagulation for treatment of diabetic retinopathy:preliminary results'. Proceedings of 30th International Symposium on Automotive Technology and Automation, Florence, Vol. 2, pp. 655–662

GOLDBAUM, M., KATZ, N., CHAUDHURI, S., and NELSON, M. (1989): 'Image understanding for automated retinal diagnosis'. Proceedings of IEEE Symposium for Computer Applications in Clinical Medicine, pp. 756–760

GOLDBAUM, M., KATZ, N., CHAUDHURI, M., NELSON, M., and KUBE, P. (1990*a*): 'Digital image processing for ocular fundus images', *Ophthalmol. Clin. North Am.*, **3**, pp. 447–466

GOLDBAUM, M., KATZ, N., NELSON, M., and HAFF, L. (1990*b*): 'The discrimination of similarly colored objects in computer images of the ocular fundus', *Invest. Ophthal. Vis. Sci.*, **31**, pp. 617–623

GOLDBAUM, M., KOUZNETSOVA, V., COTE, B., HART, W., and NELSON, M. (1993): 'Automated registration of digital ocular fundus images for comparison of lesions', *SPIE: Ophthalmic Technol. III*, **1877**, pp. 94–99

GOLDBAUM, M., JAIN, R., GUPTA, A., MOEZZI, S., TAYLOR, A., CHATTERJEE, S., and BURGESS, S. (1996): 'Database for ocular fundus images ranked by semantic similarity', *Investigat. Ophthalmol. Vis. Sci.*, **37**, p. S957

GONZALEZ, R., and WOODS, R. (1992): 'Digital image processing' (Addison-Wesley, 1992)

GREGSON, P., SHEN, Z., SCOTT, R., and KOZOUDEK, V. (1995): 'Automated grading of venous beading', *Comput. Biomed. Res.*, **28**, pp. 291–304

HAMMER, M., LEISTRITZ, S., LEISTRITZ, L., SCHWEITSER, D., THAMM, E., and DONNERHACKE, K. H. (1997): 'Monte-Carlo simulation of retinal vessel profiles for the interpretation of *in vivo* oxymetric measurements by imaging fundus reflectometry'. Proceedings on Medical Applications of Lasers in Dermatology, Ophthalmology, Dentistry, and Endoscopy, San Remo, Italy, Vol. 3192, pp. 211–218

HART, W., GOLDBAUM, M., COTE, B., KUBE, P., and NELSON, M. (1997): 'Automated measurement of retinal vascular tortuosity'. Proceedings of American Medical Informatics Association Annual Fall Symposium, Nashville, Vol. 63, pp. 459–463

HENRICSSON, M., KARLSON, C., EKHOLM, L., KAIKKONEN, P., SELLMAN, A., STEFFERT, E., and TYRBERG, M. (2000): 'Colour slides or digital photography in diabetes screening—a comparison', *Acta Ophthalmologica Scand.*, **78**, pp. 164–168

HIPWELL, J., STRACHNT, F., OLSON, J., MCHARDY, K., SHARP, P., and FORRESTER, J. (2000): 'Automated detection of microaneurysms in digital red-free photographs: a diabetic retinopathy screening tool', *Diabet. Med.*, **17**, pp. 588–594

HOOVER, A., and GOLDBAUM, M. (1998*a*): 'Fuzzy convergence'. Proceedings of IEEE Computer Society Conference on Computer Vision and Pattern Recognition, Santa Barbara, California, pp. 716–721

HOOVER, A., KOUZNETSOVA, V., and GOLDBAUM, M. (1998*b*): 'Location blood vessels in retinal images by piece-wise threshold probing of a matched filter response', American Medical Informatics Association Conference, Orlando, pp. 931–935

IIOOVER, A., KOUZNETZOVA, V., and GOLDBAUM, M. (2000): 'Locating blood vessels in retinal images by piece-wise threshold probing of a matched fileter response', *IEEE Trans. Med. Imaging.*, **19**, pp. 203–210

HUNTER, A., LOWELL, J., OWENS, J., KENNEDY, L., and STEELE, D. (2000): 'Quantification of diabetic retinopathy using neural networks and sensitivity analysis'. Proceedings of Artificial Neural Networks in Medicine and Biology, Götenborg, Sweden, pp. 81–86

ILIASOVA, N., USTINOV, A., BRANCHEVSKY, S., and DURASOV, A. (1998): 'Methods for estimating geometric parameters of retinal vessels using diagnostic images of fundus'. Proceedings of SPIE Conference on Optical Information Science and Computer and Holographic Optics and Image Processing, **3460**, pp. 316–325

JASIOBEDSKI, P., TAYLOR, C., and BRUNT, J. (1993): 'Automated analysis of retinal images', *Image Vision Comput.*, **11**, pp. 139–144

JAVITT, J., AIELLO, L., CHIANG, Y., FERRIS, F., CANNER, J., and GREENFIELD, S. (1994): 'Preventive eye care in people with diabetes is cost-saving to the federal government', *Diabetes Care*, **17**, pp. 909–917

KATZ, N., GOLDBAUM, M., NELSON, M., and CHAUDHURI, S. (1988): 'An image processing system for automatic retina diagnosis'. Proceedings of SPIE Conference on Three-Dimensional Imaging and Remote Sensing Imaging, pp. 131–137

KLEIN, R., KLEIN, B., MAGLI, Y., BROTHERS, R., MEUER, S., MOSS, S., and DAVIS, M. (1986): 'An alternative method of grading diabetic retinopathy', *Ophthalmology*, **93**, pp. 1183–1187

KLEIN, R., MOSS, S., KLEIN, B., DAVIS, M., and DEMETS, D. (1989): 'The Wisconsin epidemiologic study of diabetic retinopathy: XI The incidence of macular edema', *Ophthalmology*, **96**, pp. 1501–1510

KOCHNER, B., SCHULMAN, D., OBERMAIER, M., ZAHLMANN, G., MANN, G., and ENGLMEIER, K. H. (1997): 'An image processing system for analysing color fundus photographs with regard to diabetic retinopathy', *Klinische Monatsblatter fur Augenheilkunde*, **211**, p. 11

KOCHNER, B., SCHUHMANN, D., MICHAELIS, M., MANN, G., and ENGLEMEIER, K.-H. (1998): 'Course tracking and contour extraction of retinal vessels from color fundus photographs: most efficient use of steerable filters for model based image analysis'. Proceedings of SPIE Conference on Medical Imaging, pp. 755–761

KOZOUSEK, V., SHEN, Z., GREGSON, P., and SCOTT, R. (1992): 'Automated detection and quantification of venous beading using fourier analysis', *Can. J. Ophthalmol.*, **27**, pp. 288–294

KRISTINSSON, J., GOTTFREDSDOTTIR, M., and STEFANSSON, E. (1997): 'Retinal vessel dilation and elongation precedes diabetic macular oedema', *Br. J. Ophthalmol.*, **81**, pp. 274–278

LANDINI, G., MISSON, G., and MURRAY, P. (1993): 'Fractal analysis of the normal human retinal flourescin angiogram', *Current Eye Res.*, **12**, pp. 23–27

LANDINI, G., MURRAY, P., and MISSON, C. (1995): 'Local connected fractal dimensions and lacunarity analysis of 60 fluorecin angiograms', *Investigat. Ophthalmol. Visual Sci.*, **36**, pp. 2749–2755

LEE, S. (1992): 'Identifying retinal vessel networks in ocular fundus images'. PhD thesis, The University of New Mexico, USA

LEE, S., and WANG, Y. (1998): 'A general algorithm of recognizing small, vague and imager-alike objects in a nonuniformly illuminated medical diagnostic image'. Proceedings of 32nd Conference on Signals Systems and Computers, **2**, Asilomar, pp. 941–943

LEE, S., and WANG, Y. (1999): 'Automatic retinal image quality assessment and enhancement'. SPIE Conference on Image Processing, **3661**, pp. 1581–1590

LEE, S., WANG, Y., and LEE, E. (1999): 'A computer algorithm for automated detection and quantification of microanuerysms and hemorrhages (hma's) in color retinal images'. SPIE Conference on Image Perception and Performance, **3663**, pp. 61–71

LIESENFELD, B., KOHNER, E., PIEHLMEIER, W., KLUTHE, S., PORTA, M., BEK, T., OBERMAIER, M., MAYER, H., MANN, G., HOLLE, R., and HEP, K. (2000): A telemedical approach to the screening of diabetic retinopathy: Digital fundus photography', *Diabetes Care*, **23**, pp. 345–348

MARTÍNEZ-PÉREZ, M., HUGHES, A., STANTON, A., THOM, S., BHARATH, A., and PARKER, K. (1999*a*): 'Segmentation of retinal blood vessels based on the second directional derivative and region growing'. Proceedings of International Conference on Image Processing, New Jersey, USA, pp. 173–176

MARTÍNEZ-PÉREZ, M., HUGHES, A., STANTON, A., THOM, S., BHARATH, A., and PARKER, K. (1999*b*): 'Retinal blood vessel segmentation by means of scale-space analysis and region growing'. Proceedings of 2nd International Conference on Medical Image Computing and Computer Assisted Intervention, Cambridge, UK, pp. 90–97

MENDONÇA, A., CAMPILHO, A., and NUNES, J. (1999): 'Automatic segementation of microaneurysms in retinal angiograms of diabetic patients'. Proceedings of 10th International Conference on Image Analysis and Processing, Los Alamitos, pp. 728–723

NATIONAL SCREENING COMMITTEE (2000): 'Second report of the United Kingdom national screening committee'. Department of Health, PO Box 777, London SE1 6XH, United Kindom.

NGUYEN, H., BUTTLER, M., ROYCHOUDHRY, A., SHANNON, A., FLACK, J., and MITCHEL, P. (1996): 'Classification of diabetic retinopathy using neural networks'. Proceedings of 18th Annual International Conference of IEEE Engineering in Medicine and Biology Society, IEEE, Amsterdam, The Netherlands, Vol. 4, pp. 1548–1549

ØIEN, G., and OSNES, P. (1995): 'Diabetic retinopathy: Automatic detection of early symptoms from retinal images'. Proceedings of Norwegian Signal Processing Symposium, Stavanger, Norway, Vol. VII, pp. 135–140
OKAZAKI, K., and TAMURA, S. (1983): 'Spherical shading correction of eye fundus image'. Proceedings of International Conference on Systems, Man and Cybernetics, Bombay, India, pp. 1084–1087
OTSU, N. (1979): 'A threshold method from gray-level histograms', *IEEE Trans. Syst. Man Cybern.*, **9**, pp. 62–66
PANICO, J., and STERLING, P. (1995): 'Retinal neurons and vessels are not fractal but space-filling', *J. Compar. Neurol.*, **361**, pp. 479–490
PATEL, V. (1995): 'Diabetic retinopathy: haemodynamic and clinical factors in the pathogenesis' (Verlag, Josef Eul, Koln, 1995 (ISBN): 3-89012-432-1)
PELI, E. (1993): 'Enhancement of retinal images: Pros and problems', *Neurosci. Biobehav. Rev.*, **17**, pp. 477–482
PHILLIPS, R., SPENCER, T., ROSS, P., SHARP, P., and FORRESTER, J. (1991): 'Quantification of diabetic maculopathy by digital imaging of the fundus', *Eye*, **5**, pp. 130–137
POLI, R., and VALLI, G. (1997): 'An algorithm for real-time vessel enhancement and detection', *Comput. Methods Programs Biomed.*, **52**, pp. 1–22
RASSAM, S., PATEL, V., BRINCHMANN-HANSEN, O., ENGVOLD, O., and KOHNER, E. (1994): 'Accurate vessel width measurement from fundus photographs: a new concept', *Br. J. Ophthalmol.*, **78**, pp. 24–29
RYAN, N., and HENEGHAN, C. (1999): 'Image registration techniques for digital ophthalmic images'. Irish Signal and Systems Conference, Galway, Ireland, pp. 301–308
SCHALKOFF, R. (1989): '*Digital image processing and computer vision*' (Wiley and Sons, Inc., New York, 1989)
SCOTT, J., FISHER, R., and PALMER, E. (1996): 'Neural networks in ventilation-perfusion imaging; part ii. Effects of interpretive variability', *Radiology*, **198**, pp. 707–713
SHIN, D., KAISER, R., LEE, M., and BERGER, J. (1999): 'Fundus image change analysis:geometric and radiometric normalisation'. Proceedings of SPIE Conference on Ophthalmic Technologies, **3591**, San Jose, California, pp. 129–136
SINCLAIR, S., GUPTA, A., and BHASIN, S. (1996): 'Automated lesion detection and grading of retinopathy from fundus photographs of diabetics', *Diabetes*, **45**, p. 192A
SINTHANAYOTHIN, C., BOYCE, J., COOK, H., and WILLIAMSON, T. (1999): 'Automated localisation of the optic disk, fovea, and retinal blood vessels from digital colour fundus images', *Br. J. Ophthalmol.*, **83**, pp. 902–910
SKOVBORG, F., NIELSEN, A., LAURITZEN, E., and HARKTOPP, O. (1969): 'Diameters of the retinal vessels in diabetic and normal subjects', *Diabetes*, **18**, pp. 292–298
SOLIZ, P., NEMETH, S., SWIFT, M., EDWARDS, A., MEUER, S., and BERGER, J. (2000): 'Improving the visualisation of drusen in age-related macular degeneration through maximum entropy digitization and stereo viewing'. Proceedings of SPIE Conference on Medical Imaging 2000: Image Perception and Performance, **3981**, pp. 217–281
SPENCER, T., OLSON, J., SHARP, P., and FORRESTER, J. (1994): 'A 'region-growing' approach to the quantification of microaneurysms in the diabetic retina'. BES/IPSM Meeting Engineering and Technology in Diabetes, Bournemouth, United Kingdom, p. 12
SPENCER, T., OLSON, J., MCHARDY, K., SHARP, P., and FORRESTER, J. (1996): 'An image-processing strategy for the segmentation and quantification of microaneurysms in flourescein angiograms of the ocular fundus', *Comput. Biomed. Res.*, **29**, pp. 284–302
TAMURA, S., OKAMOTO, Y., and YANASHIMA, K. (1988): 'Zero-crossing interval correction in tracing eye-fundus blood vessels', *Pattern Recognit.*, **21**, pp. 227–233
TANAKA, M., and TANAKA, K. (1988): 'An automatic technique for fundus-photograph mosaic and vascular net reconstruction'. Proceedings of MEDINFO, pp. 116–120
THOMPSON, H. (1999): 'A wavelet-based method for automated computer detection of diabetic retinopathy in fundus photographs', *Invest. Opthal. Visual Science*, **40**, p. S121
TOLIAS, Y., and PANAS, S. (1998): 'A fuzzy vessel tracking algorithm for retinal images based on fuzzy clustering', *IEEE Trans. Med. Imaging*, **17**, pp. 263–273
WANG, Y., and LEE, S. (1997): 'A fast method for automated detection of blood vessels in retinal images'. Asilomar Conference, IEEE Computer Society, Pacific Grove, CA, Vol. 2, pp. 1700–1704
WANG, Y., TOONEN, H., and MEYER-EBRECHT, D. (1990): 'A new method of automatic tracking, measuring blood vessels in retinal image'. Annual International Conference of IEEE Engineering in Medicine and Biology Society, Vol. 12, Philadelphia, USA, pp. 174–175
WARD, N., TOMLINSON, S., and TAYLOR, C. (1988): 'Image analysis of fundus photographs', *Ophthalmology*, **96**, pp. 80–86
WEST, G., BROWN, J., and ENQUIST, B. (1997): 'A general model for the origin of allometric scalling laws in biology', *Science*, **276**, pp. 122–126
WOOD, S. (1990): 'Analysis of retinal vessel structure from multiple images'. Annual International Conference of IEEE Engineering in Medicine and Biology Society, Vol. 12, Philadelphia, pp. 176–177
YANG, C.-W., MA, D.-J., WANG, C.-M., WEN, C.-H., LO, C.-S., and CHANG, C.-I. (2000): 'Computer-aided diagnostic detection system of venous beading in retinal images', *Opt. Eng.*, **39**, pp. 1293–1303
YE, D., and ZHENG, L. (1995): 'Fundus image processing and feature classification based on mathematical morphology method'. Proceedings of the Canadian Medical and Biological Engineers Conference, Vol. 2, pp. 1015–1016
YOUNG, S., GEORGE, L., LUSTY, J., and OWENS, D. (1997): 'A new screening tool for diabetic retinopathy: the Canon CR5 45NM retinal camera with Frost Medical Software RIS-Lite digital imaging system', *J. Audiovisual Media Med.*, **20**, pp. 11–14
YU, J., HUNG, B., and SUN, H. (1990): 'Automatic recognition of retinopathy from retinal images'. Proceedings of Twelfth Annual International Conference on IEEE Engineering and Medicine and Biology Society, Philadelphia, Vol. 12, pp. 171–173
YULONG, M., and DINGRU, X. (1990): 'Recognizing the glaucoma from ocular fundus image by image processing'. Proceedings of Twelfth Annual International Conference of the IEEE Engineering in Medicine and Biology Society, Philadelphia, Vol. 12, pp. 178–179
ZAHLMANN, G., SCHUBERT, M., OBERMAIER, M., and MANN, G. (1996): 'Concept of a knowledge based monitoring system for glaucoma and diabetic retinopathy using a telemedicine approach'. 18th Annual International Conference of the IEEE Engineering in Medicine and Biology Society, Amsterdam, pp. 1230–1231
ZAHLMANN, G., KOCHNER, B., UGI, I., SCHULHMANN, D., LIESENFELD, B., WEGNER, A., OBERMAIER, M., and MERTZ, M. (2000): 'Hybrid fuzzy image processing for situation assessment: A knowledge-based system for early detection of diabetic retinopathy', *IEEE Eng. Med. Biol.*, **19**, pp. 76–83
ZHOU, L., RZESZOTARSKI, M., SINGERMAN, L., and CHOKREFF, J. (1994): 'The detection and quantification of retinopathy using digital angiograms', *IEEE Trans. Med. Imag.*, **13**, 619–626

Authors' biographies

THOMAS TENG received his BSc in Medical Instrumentation and Computing from Bournemouth University in 1997. He is currently undertaking research into the development and application of intelligent systems for medical image processing.

MARTIN LEFLEY is a reader in intelligent interfaces at Bournemouth University. He has a Masters in Statistics from Newcastle University and was awarded his PhD for utilising computer vision in knitted fabric inspection, in 1988. He is investigating the practical applications of artificial intelligence. Many of these projects used neural networks to realise computer visual abilities.

DENZIL CLAREMONT is Professor of Biomedical Engineering at Bournemouth University. He received a BSc honours degree in Physiology from the University of London in 1975, an MSc in Bioengineering from Strathclyde University in 1976 and a DPhil from Sussex University in 1981. His research interests include physiological measurements and in the development and application of engineering in the management of diabetes.